Supplementary Materials

Anion photoelectron spectroscopy and density functional theory study of $TM_2Si_n^-$ (TM= V, Cr; n = 14–20) clusters†

Kai Wang, ‡[a] Guang-Jia Yin,‡[a] Ze-Zhao Jia,[a] Lin Miao,[a] Ramiro Moro,[a] Bernd von Issendorff [b] and Lei Ma*[a]

[1]*Tianjin International Center for Nanoparticles and Nanosystems, Tianjin University, 92 Weijin Road, Nankai District, Tianjin 300072, China.*

[2] *Fakultät für Physik, Universität Freiburg, H. Herderstr. 3. D-79104 Freiburg, Germany*

[a)] *Authors to whom correspondence should be addressed: E-mail:* lei.ma@tju.edu.cn

‡ These authors contributed equally

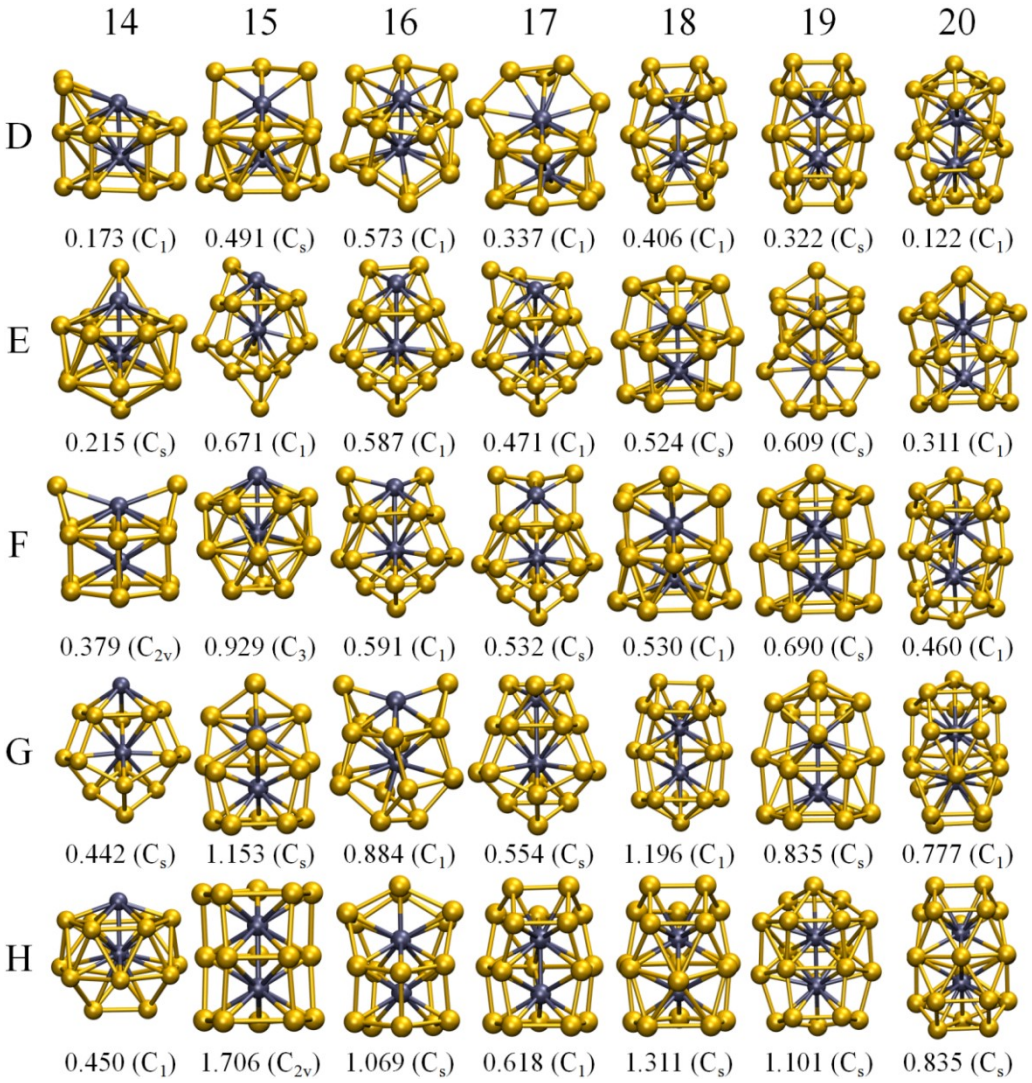

Fig. S1. Low-lying structures of $V_2Si_n^-$ (*n* = 14−20) clusters. For each structure, the total energy difference (eV) with respect to the lowest-energy isomer shown in the main text as obtained at the BP86/TZVPD level and the symmetry are given. Grey and golden balls represent V and Si atoms, respectively.

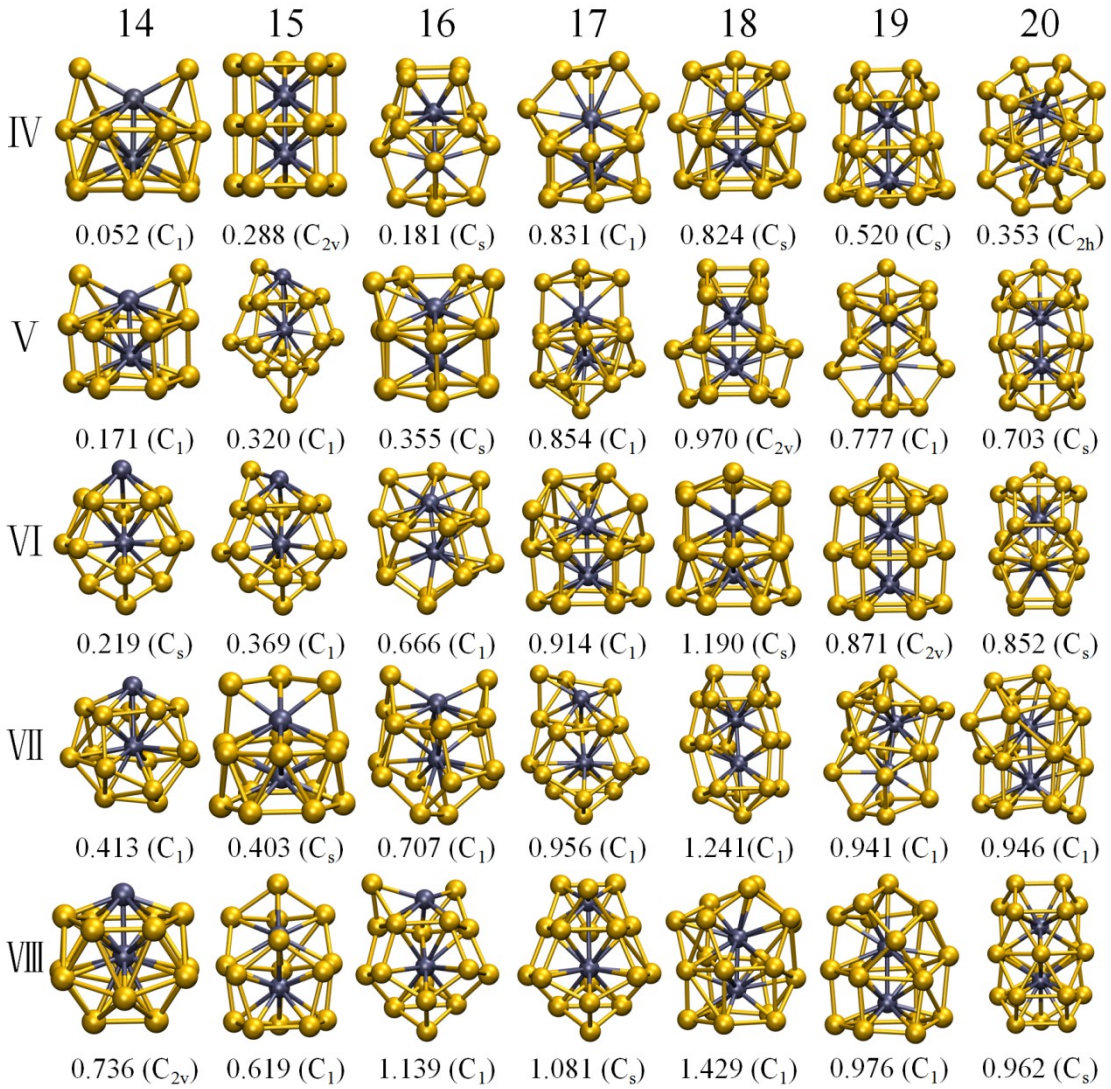

Fig. S2. Low-lying structures of $Cr_2Si_n^-$ (*n* = 14−20) clusters. For each structure, the total energy difference (eV) with respect to the lowest-energy isomer in the main text as obtained at the BP86/TZVPD level and the symmetry are given. Grey and golden balls represent Cr and Si atoms, respectively.

Table S1. Experimentally (Expt.) measured VDEs and those theoretical predicted ones using seven different functionals for the structures which are optimized at the def2-TZVP level and calculated at def2-TZVPD level. All energies are given in eV. The uncertainties of the experimental VDEs are shown in the parentheses. The SD is the standard deviation of VDE for a given functional.

VDE (eV)

Clusters	PBE	BLYP	BP86	PBE0	M06	M06-2X	B3P	Expt.
$V_2Si_{14}^-$	3.05	2.80	3.13	3.26	3.02	3.37	3.29	3.21(3)
$V_2Si_{15}^-$	3.47	3.20	3.54	3.64	3.46	3.65	3.70	3.59(3)
$V_2Si_{16}^-$	3.76	3.54	3.74	3.88	3.70	3.95	3.91	3.83(3)
$V_2Si_{17}^-$	3.02	2.80	3.09	3.33	2.99	3.77	3.35	3.12(3)
$V_2Si_{18}^-$	3.46	3.12	3.54	3.49	3.68	3.78	3.58	3.53(3)
$V_2Si_{19}^-$	3.43	3.16	3.50	3.80	3.55	3.79	3.86	3.59(3)
$V_2Si_{20}^-$	3.43	3.17	3.50	3.58	3.52	3.76	3.54	3.57(3)
$Cr_2Si_{14}^-$	3.06	2.91	3.16	2.98	2.98	3.04	3.10	3.12(3)
$Cr_2Si_{15}^-$	3.06	2.83	3.12	2.79	2.73	3.15	2.92	3.13(3)
$Cr_2Si_{16}^-$	3.01	2.77	3.08	3.79	3.69	3.53	3.87	3.13(3)
SD	0.11	0.36	0.06	0.26	0.25	0.28	0.27	

TABLE S2. Experimental (Expt.) and theoretical vertical detachment energies (VDEs) of the putative ground-state structures shown in the main text, calculated with seven different functionals. The def2-TZVP basis set was used for structure optimization, further energy calculation adopt def2-TZVPD as the basis set. The "Unopt" column indicates results for putative ground state structures obtained with the BP86 functional, while the "opt" column shows the results for the same structures, but relaxed using the listed functional.

Cluster	VDE (eV)						
	PBE		BLYP		PBE0		Expt.
	Unopt	opt	Unopt	opt	Unopt	opt	
$V_2Si_{14}^-$	3.06	3.05	2.78	2.80	3.31	3.26	3.21(3)
$V_2Si_{15}^-$	3.47	3.47	3.19	3.20	3.65	3.64	3.59(3)
$V_2Si_{16}^-$	3.68	3.76	3.38	3.54	3.90	3.88	3.83(3)
$V_2Si_{17}^-$	3.02	3.02	2.74	2.80	3.37	3.33	3.12(3)
$V_2Si_{18}^-$	3.46	3.46	3.22	3.12	3.58	3.49	3.53(3)
$V_2Si_{19}^-$	3.43	3.43	3.16	3.16	3.76	3.80	3.59(3)
$V_2Si_{20}^-$	3.43	3.43	3.17	3.17	3.61	3.58	3.57(3)
$Cr_2Si_{14}^-$	3.09	3.06	2.83	2.91	3.13	2.98	3.12(3)
$Cr_2Si_{15}^-$	3.06	3.06	2.82	2.83	2.82	2.79	3.13(3)
$Cr_2Si_{16}^-$	3.01	3.01	2.75	2.77	3.77	3.79	3.13(3)

TABLE S3. Average Si – Si and TM – Si bond lengths in isomer nA of the $TM_2Si_n^-$ (TM=V, Cr; n = 14 – 20) cluster anions by using five different functionals by using the def2-TZVP basis set.

Cluster	Bond length (Å)									
	BP86		PBE		BLYP		PBE0		B3P	
	Si-Si	TM-Si	Si-Si	TM-Si	Si-Si	TM-Si	Si-Si	TM-Si	Si-Si	TM-Si
$V_2Si_{14}^-$	2.48	2.65	2.47	2.65	2.51	2.68	2.45	2.63	2.46	2.64
$V_2Si_{15}^-$	2.49	2.64	2.48	2.64	2.52	2.68	2.46	2.62	2.47	2.62
$V_2Si_{16}^-$	2.47	2.68	2.47	2.64	2.51	2.68	2.45	2.66	2.46	2.67
$V_2Si_{17}^-$	2.49	2.69	2.48	2.68	2.52	2.70	2.46	2.67	2.47	2.68
$V_2Si_{18}^-$	2.37	2.65	2.36	2.65	2.39	2.70	2.34	2.63	2.35	2.63

$V_2Si_{19}^-$	2.41	2.70	2.40	2.70	2.44	2.74	2.40	2.68	2.39	2.68
$V_2Si_{20}^-$	2.39	2.70	2.38	2.69	2.39	2.74	2.36	2.67	2.35	2.70
$Cr_2Si_{14}^-$	2.36	2.65	2.36	2.64	2.39	2.65	2.37	2.69	2.35	2.69
$Cr_2Si_{15}^-$	2.42	2.68	2.41	2.67	2.42	2.71	2.41	2.69	2.41	2.69
$Cr_2Si_{16}^-$	2.47	2.65	2.46	2.64	2.50	2.68	2.45	2.67	2.46	2.67
$Cr_2Si_{17}^-$	2.40	2.57	2.39	2.57	2.42	2.61	2.38	2.59	2.38	2.59
$Cr_2Si_{18}^-$	2.35	2.66	2.35	2.65	2.37	2.69	2.34	2.65	2.36	2.64
$Cr_2Si_{19}^-$	2.35	2.66	2.34	2.65	2.37	2.68	2.37	2.64	2.37	2.65
$Cr_2Si_{20}^-$	2.40	2.69	2.39	2.68	2.41	2.74	2.39	2.70	2.39	2.70

TABLE S4. TM-TM bond length in isomer nA of the $TM_2Si_n^-$ (TM=V, Cr; n = 14 – 20) cluster anions by using five different functionals by using the def2-TZVP basis set.

Cluster	TM-TM bond length (Å)				
	BP86	PBE	BLYP	PBE0	B3P
$V_2Si_{14}^-$	2.33	2.33	2.35	2.33	2.33
$V_2Si_{15}^-$	2.33	2.33	2.35	2.31	2.32
$V_2Si_{16}^-$	2.35	2.34	2.35	2.32	2.31
$V_2Si_{17}^-$	2.35	2.34	2.38	2.36	2.35
$V_2Si_{18}^-$	2.46	2.45	2.43	2.46	2.46
$V_2Si_{19}^-$	2.73	2.73	2.69	2.85	2.81
$V_2Si_{20}^-$	2.46	2.47	2.47	2.47	2.46
$Cr_2Si_{14}^-$	2.17	2.18	2.18	2.55	2.51
$Cr_2Si_{15}^-$	2.20	2.20	2.20	2.39	2.36
$Cr_2Si_{16}^-$	2.27	2.27	2.29	2.43	2.39
$Cr_2Si_{17}^-$	2.32	2.32	2.33	2.37	2.36
$Cr_2Si_{18}^-$	2.32	2.32	2.33	2.40	2.37
$Cr_2Si_{19}^-$	2.40	2.40	2.38	2.48	2.46
$Cr_2Si_{20}^-$	2.55	2.55	2.54	2.65	2.64

TABLE S5. Average binding energies (Eb) and HOMO-LUMO gaps (Gap) of the isomer nA of the $TM_2Si_n^-$ (TM=V, Cr; n = 14 – 20) cluster anions by using five different functionals by using the def2-TZVPD basis set. The unit of energy is eV.

Cluster	BP86		PBE		BLYP		PBE0		B3P	
	Eb	Gap	Eb	Gap	Eb	Gap	Eb	Gap	Eb	Gap
$V_2Si_{14}^-$	4.034	0.303	3.240	0.294	3.636	0.258	3.919	1.531	3.803	1.289
$V_2Si_{15}^-$	4.037	0.463	3.229	0.440	3.638	0.384	3.938	1.930	3.819	1.630
$V_2Si_{16}^-$	4.039	0.332	3.215	0.261	3.629	0.185	3.948	1.701	3.826	1.413
$V_2Si_{17}^-$	4.025	0.541	3.199	0.517	3.619	0.518	3.955	2.061	3.825	1.784
$V_2Si_{18}^-$	4.056	0.262	3.204	0.254	3.680	0.208	3.984	1.367	3.869	1.128
$V_2Si_{19}^-$	4.049	0.375	3.199	0.358	3.653	0.288	3.993	1.894	3.864	1.654
$V_2Si_{20}^-$	4.053	0.194	3.190	0.186	3.666	0.169	3.996	1.285	3.874	1.220

$Cr_2Si_{14}^-$	3.748	0.279	2.933	0.261	3.433	0.269	3.632	1.275	3.530	1.075
$Cr_2Si_{15}^-$	3.771	0.368	2.951	0.339	3.437	0.395	3.652	1.308	3.547	1.163
$Cr_2Si_{16}^-$	3.793	0.505	2.968	0.497	3.441	0.520	3.661	1.609	3.549	1.452
$Cr_2Si_{17}^-$	3.810	0.235	2.964	0.229	3.475	0.196	3.686	1.444	3.584	1.218
$Cr_2Si_{18}^-$	3.855	0.451	2.998	0.430	3.519	0.400	3.750	0.942	3.643	0.784
$Cr_2Si_{19}^-$	3.845	0.255	2.983	0.241	3.504	0.250	3.769	1.491	3.656	1.267
$Cr_2Si_{20}^-$	3.853	0.216	2.990	0.208	3.495	0.190	3.775	1.447	3.657	1.227

TABLE S6. The second order difference in energy (Δ^2E) in isomer nA of the $TM_2Si_n^-$ (TM=V, Cr; n = 14 – 20) cluster anions by using five different functionals by using the def2-TZVPD basis set. The unit of energy is eV.

Cluster	Δ^2E (eV)				
	BP86	PBE	BLYP	PBE0	B3P
$V_2Si_{14}^-$	--	--	--	--	--
$V_2Si_{15}^-$	0.025	0.070	0.209	0.105	0.139
$V_2Si_{16}^-$	0.289	0.079	0.035	0.060	0.130
$V_2Si_{17}^-$	-0.859	-0.385	-1.412	-0.464	-0.900
$V_2Si_{18}^-$	0.721	0.187	1.742	0.352	0.948
$V_2Si_{19}^-$	-0.218	0.094	-0.836	0.107	-0.312
$V_2Si_{20}^-$	--	--	--	--	--
$Cr_2Si_{14}^-$	--	--	--	--	--
$Cr_2Si_{15}^-$	-0.021	-0.041	-0.004	0.166	0.206
$Cr_2Si_{16}^-$	0.038	0.388	-0.567	-0.319	-0.605
$Cr_2Si_{17}^-$	-0.582	-0.765	-0.287	-0.836	-0.572
$Cr_2Si_{18}^-$	1.050	0.957	1.165	0.813	0.872
$Cr_2Si_{19}^-$	-0.346	-0.041	-0.121	0.243	0.230
$Cr_2Si_{20}^-$	--	--	--	--	--

TABLE S7. On-site spin moment on the top TM atom and bottom TM atom in isomer nA of the $TM_2Si_n^-$ (TM=V, Cr; n = 14–20) cluster anions from Hirshfeld population analysis by using five different functionals. The structures have been optimized using BP86 and the def2-TZVP basis set, for the calculations the basis set def2-TZVPD was used. μTM-top and μTM-bottom denote the magnetic moments of the upper TM atom and the lower TM atom (see Fig. 8), respectively.

Cluster	Magnetic moment (μB)									
	BP86		PBE		BLYP		PBE0		B3P	
	μ_{TM}-top	μ_{TM}-bottom	μ_{TM}-top	μ_{TM}-bottom	μ_{TM}-top	μ_{TM}-bottom	μ_{TM}-top	μ_{TM}-bottom	μ_{TM}-top	μ_{TM}-bottom
$V_2Si_{14}^-$	0.257	0.039	0.251	0.045	0.245	0.046	0.937	-0.714	0.695	-0.430
$V_2Si_{15}^-$	0.287	0.160	0.278	0.159	0.273	0.163	0.045	0.552	0.189	0.381
$V_2Si_{16}^-$	0.109	0.324	0.113	0.314	0.106	0.310	-0.676	0.988	-0.350	0.769
$V_2Si_{17}^-$	0.688	-0.068	0.665	-0.060	0.652	-0.050	1.275	-0.445	1.142	-0.318
$V_2Si_{18}^-$	0.051	0.203	0.051	0.196	0.060	0.195	-0.259	0.419	-0.136	0.337

$V_2Si_{19}^-$	-0.027	0.573	-0.017	0.540	-0.007	0.534	-0.598	1.422	-0.430	1.273
$V_2Si_{20}^-$	0.085	0.018	0.081	0.020	0.086	0.028	0.845	-0.876	0.572	-0.546
$Cr_2Si_{14}^-$	0.425	-0.006	0.439	-0.012	0.361	0.028	2.912	-1.962	2.746	-1.635
$Cr_2Si_{15}^-$	1.191	-0.486	1.151	-0.459	1.085	-0.390	2.654	-2.222	2.481	-1.968
$Cr_2Si_{16}^-$	0.780	0.177	0.769	0.175	0.743	0.190	2.489	-1.793	2.194	-1.322
$Cr_2Si_{17}^-$	0.024	-0.001	0.023	-0.001	0.036	0.007	-2.090	2.017	-1.791	1.707
$Cr_2Si_{18}^-$	1.006	-0.626	0.949	-0.549	0.894	-0.460	2.447	-2.469	2.245	-2.249
$Cr_2Si_{19}^-$	0.532	-0.241	0.501	-0.222	0.454	-0.140	2.448	-2.344	2.228	-2.066
$Cr_2Si_{20}^-$	0.228	0.094	0.222	0.100	0.212	0.104	2.500	-2.452	2.278	-2.198

TABLE S8. On-site spin moment on the top TM atom and bottom TM atom in isomer *n*A of the $TM_2Si_n^-$ (TM=V, Cr; n = 14–20) cluster anions from Hirshfeld population analysis by using five different functionals. The structures have been optimized by using the def2-TZVP basis set and the given functional, for the calculations the basis set def2-TZVPD was used. $\mu_{TM\text{-}top}$ and $\mu_{TM\text{-}bottom}$ denote the magnetic moments of the upper TM atom and the lower TM atom (see Fig. 8), respectively.

Cluster	Magnetic moment (μ_B)									
	BP86		PBE		BLYP		PBE0		B3P	
	$\mu_{TM\text{-}top}$	$\mu_{TM\text{-}bottom}$	$\mu_{TM\text{-}top}$	$\mu_{TM\text{-}bottom}$	$\mu_{TM\text{-}top}$	$\mu_{TM\text{-}bottom}$	$\mu_{TM\text{-}top}$	$\mu_{TM\text{-}bottom}$	$\mu_{TM\text{-}top}$	$\mu_{TM\text{-}bottom}$
$V_2Si_{14}^-$	0.257	0.039	0.253	0.047	0.255	0.045	0.837	-0.580	0.598	-0.315
$V_2Si_{15}^-$	0.287	0.160	0.278	0.157	0.280	0.175	0.085	0.479	0.186	0.362
$V_2Si_{16}^-$	0.109	0.324	0.050	0.064	0.057	0.081	-0.547	0.858	-0.284	0.701
$V_2Si_{17}^-$	0.688	-0.068	0.660	-0.058	0.680	-0.058	1.241	-0.366	1.115	-0.271
$V_2Si_{18}^-$	0.051	0.203	0.052	0.193	0.056	0.200	-0.276	0.291	-0.171	0.270
$V_2Si_{19}^-$	-0.027	0.573	-0.016	0.535	0.013	0.467	-0.512	1.483	-0.382	1.335
$V_2Si_{20}^-$	0.085	0.018	0.086	0.020	0.086	0.038	0.712	-0.731	0.292	-0.332
$Cr_2Si_{14}^-$	0.425	-0.006	0.374	0.001	0.501	0.021	3.621	-2.045	3.509	-1.849
$Cr_2Si_{15}^-$	1.191	-0.486	1.113	-0.430	1.187	-0.461	3.010	-2.369	2.831	-2.140
$Cr_2Si_{16}^-$	0.780	0.177	0.761	0.178	0.760	0.196	3.017	-2.165	2.726	-1.806
$Cr_2Si_{17}^-$	0.024	-0.001	0.018	0.001	0.029	0.007	-2.132	2.109	-1.886	1.840
$Cr_2Si_{18}^-$	1.006	-0.626	0.920	-0.513	0.985	-0.572	2.489	-2.410	2.387	-2.185
$Cr_2Si_{19}^-$	0.532	-0.241	0.416	-0.176	0.661	-0.176	2.487	-2.467	2.345	-2.256
$Cr_2Si_{20}^-$	0.228	0.094	0.198	0.101	0.198	0.164	2.598	-	2.453	-2.278

								2.481		

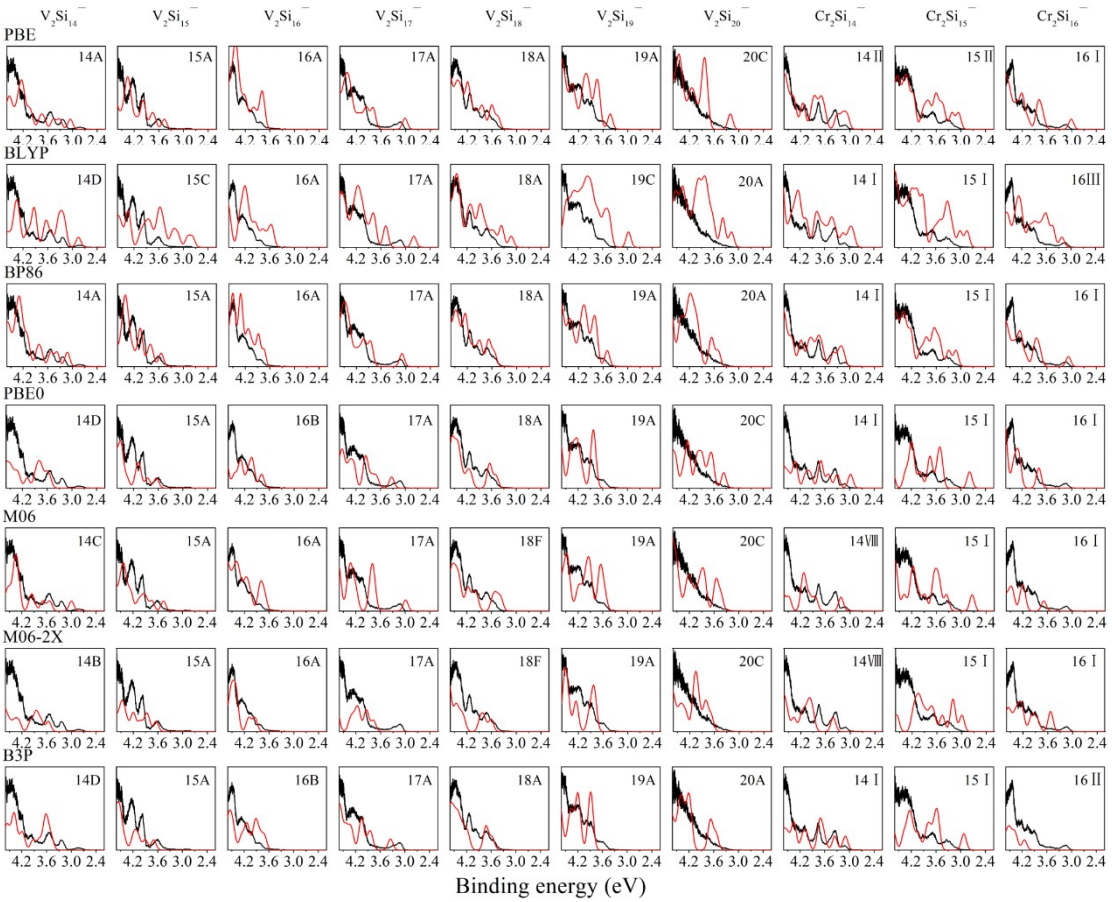

FIG. S3. Photoelectron spectra of cold (T = 10 K) $TM_2Si_n^-$ (TM=V, *n* = 14-20; TM=Cr, *n* = 14-16) cluster anions, measured at a photon energy of 5.0 eV (black lines), in comparison with the simulated photoelectron spectra (red lines) for the respective lowest energy structures (as depicted in Fig 2 in the main text and Fig. S1) using seven functionals with the def2-TZVPD basis set.

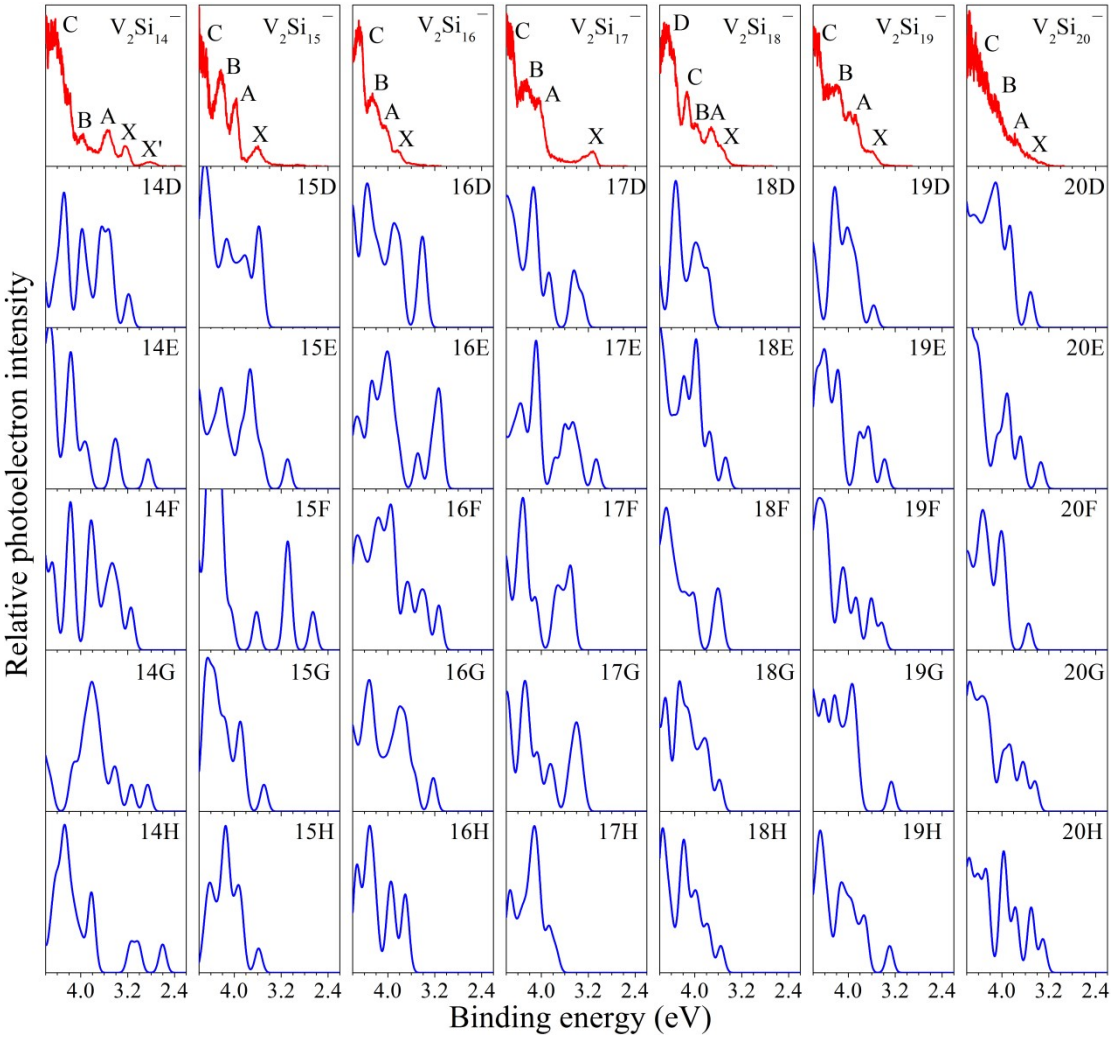

FIG. S4. Uppermost panels: experimental PES spectra of cold $V_2Si_n^-$ (n = 14–20), measured at a photon energy of 5.01 eV. Lower panels: theoretical PES spectra, calculated by density functional theory at the BP86/def2-TZVPD level for the structures shown in Fig. S1.

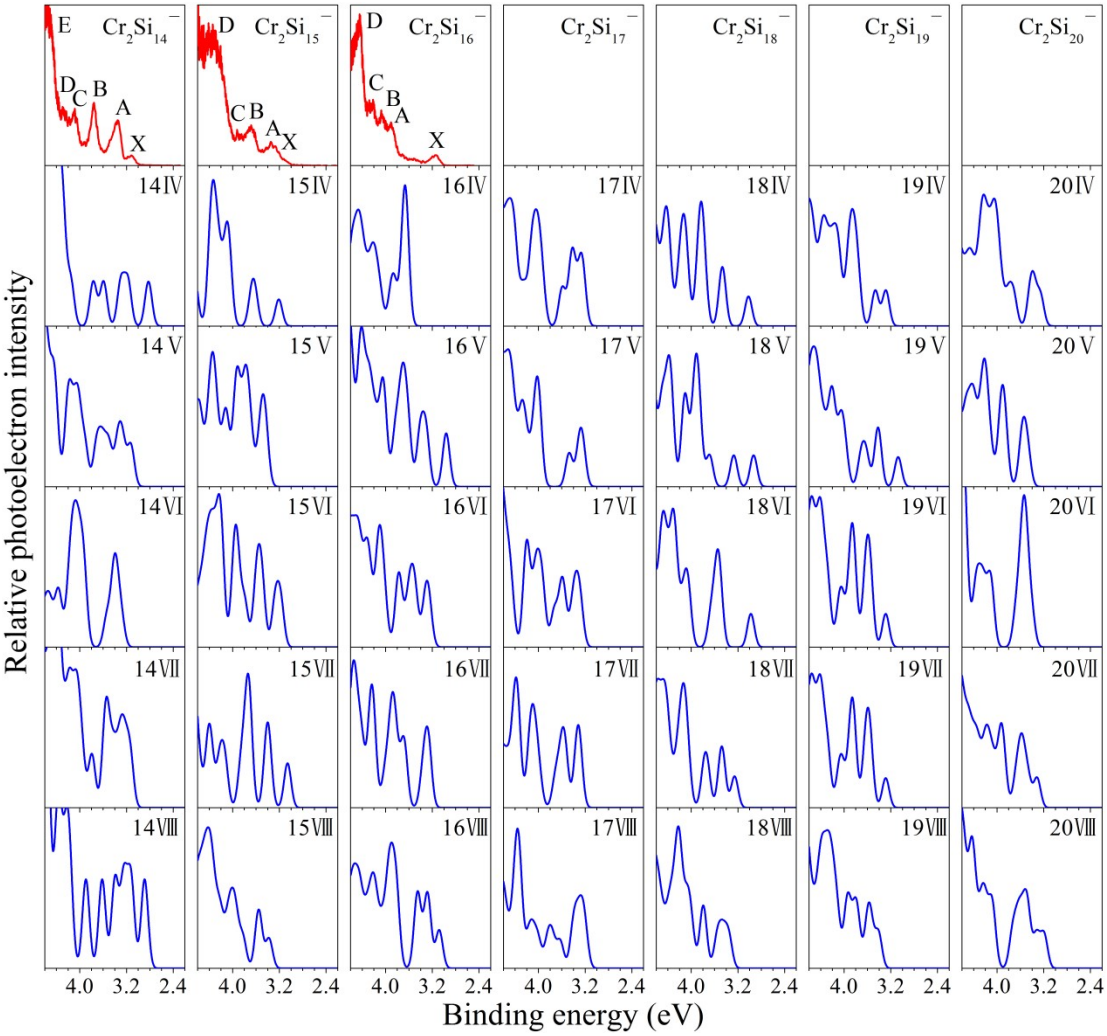

FIG. S5. Uppermost panels: experimental PES spectra of cold $Cr_2Si_n^-$ (n = 14–16), measured at a photon energy of 5.01 eV. Lower panels: theoretical PES spectra (n = 14–20), calculated by density functional theory at the BP86/def2-TZVPD level for the structures shown in Fig. S2.

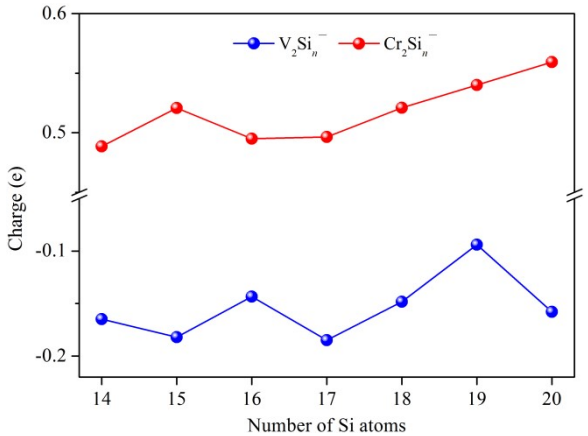

FIG. S6. Hirshfeld atomic charges on the TM_2 dimer for the TM_2Sin^- (TM=V, Cr; n = 14–20) clusters.

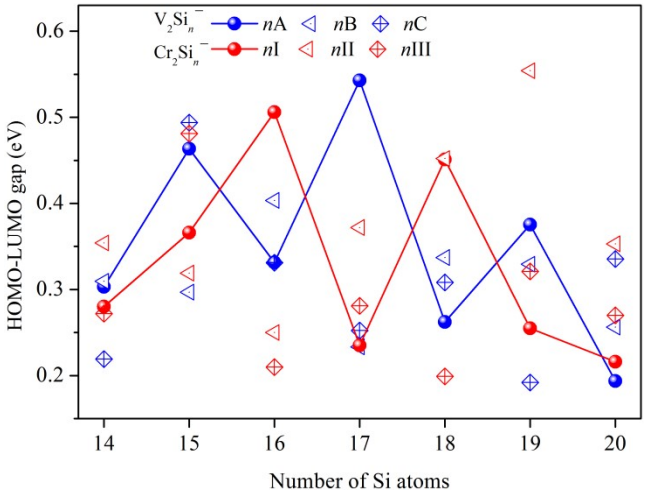

FIG. S7. HOMO-LUMO gaps of the three lowest-lying isomers of $TM_2Si_n^-$ (TM=V, Cr; n = 14–20).

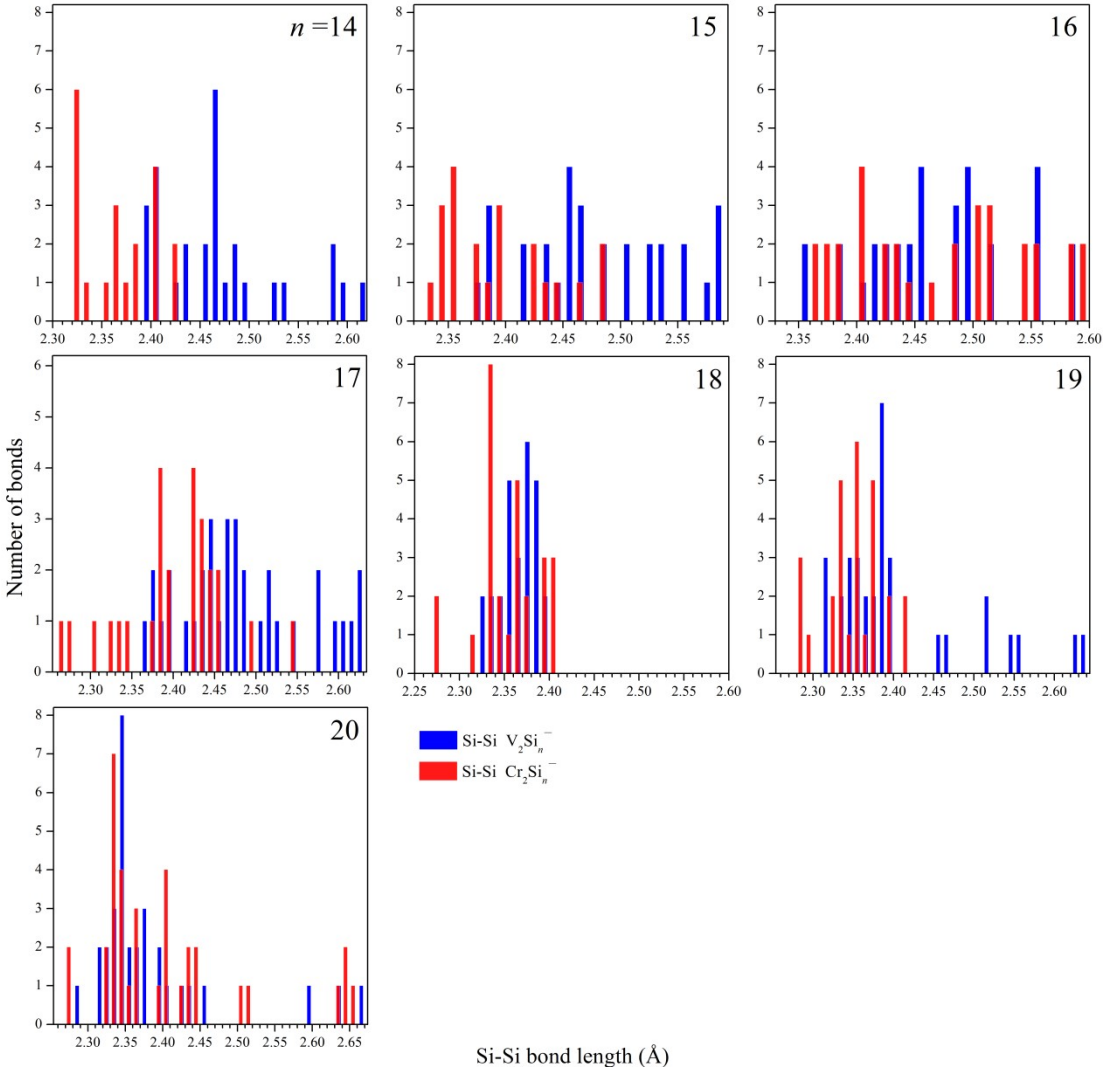

FIG. S8. The Si–Si bond length distributions of the lowest-lying isomers of $TM_2Si_n^-$ (TM=V, Cr; n = 14–20).

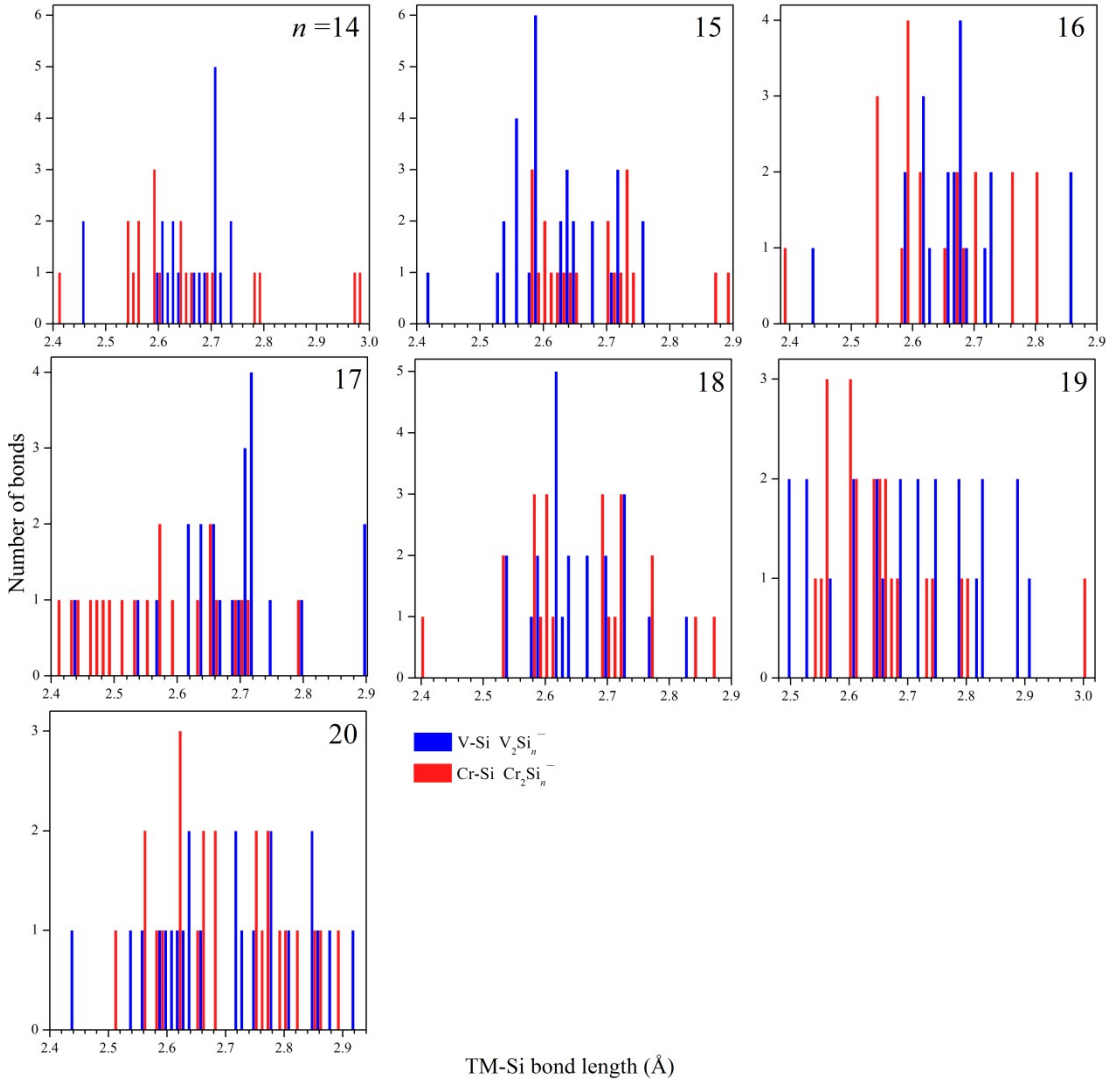

FIG. S9. The TM–Si bond length distributions of the lowest-lying isomers of $TM_2Si_n^-$ (TM=V, Cr; n = 14–20).